

# Effect of massive graviton on dark energy star structure

A. Bagheri Tudesghi<sup>1\*</sup>, G. H. Bordbar<sup>1†</sup>, and B. Eslam Panah<sup>2,3,4‡</sup>

<sup>1</sup> *Department of Physics and Biruni Observatory, Shiraz University, Shiraz 71454, Iran*

<sup>2</sup> *Department of Theoretical Physics, Faculty of Science,*

*University of Mazandaran, P. O. Box 47415-416, Babolsar, Iran*

<sup>3</sup> *ICRANet-Mazandaran, University of Mazandaran, P. O. Box 47415-416, Babolsar, Iran*

<sup>4</sup> *ICRANet, Piazza della Repubblica 10, I-65122 Pescara, Italy*

The presence of massive gravitons in the field of massive gravity is considered as an important factor in investigating the structure of compact objects. Hence, we are encouraged to study the dark energy star structure in the Vegh's massive gravity. We consider that the equation of state governing the inner spacetime of the star is the extended Chaplygin gas, and then using this equation of state, we numerically solve the Tolman-Oppenheimer-Volkoff (TOV) equation in massive gravity. In the following, assuming different values of free parameters defined in massive gravity, we calculate the properties of dark energy star such as radial pressure, transverse pressure, anisotropy parameter, and other characteristics. Then, after obtaining the maximum mass and its corresponding radius, we compute redshift and compactness. The obtained results show that for this model of dark energy star, the maximum mass and its corresponding radius depend on the massive gravity's free parameters and anisotropy parameter. These results are consistent with the observational data, and cover the lower mass gap. We also demonstrate that all energy conditions are satisfied for this model, and in the presence of anisotropy, the dark energy star is potentially unstable.

## I. INTRODUCTION

The existence of singularities in physics cannot be denied. Since a reliable physical theory must be free from these singularities, the existence of dark energy (DE) in various models, including the cosmological constant  $\Lambda$ , quintessence [1], phantom energy [2], Chaplygin gas [3], etc, in addition to providing an explanation for the accelerated expansion of the universe was an option to resolve this problem in the case of compact objects. Several attempts were made to provide the models for compact objects and the existence of dark energy in them, including the introduction of false vacuum bubbles [4], non-singular black holes [5], gravastars [6], dark energy stars (DES) [7], etc. The final stage of gravitational collapse of a compact object whose mass is greater than the mass of a neutron star, according to Chapline's proposal [7], turns into a DES in which there is no singularity in its center, and the surface of the star is introduced as a critical surface. The negative pressure created inside the star is produced by vacuum energy, which exhibits the distinction between the ground state energy of quark gas and lepton gas [8].

After the introduction of DES, due to having very large vacuum energy in the center and the occurrence of phase transition on the surface, the presence of anisotropic pressure in it was investigated in several studies. Also, the non-establishment of the hydrostatic equilibrium regarding the isotropic pressure in gravastars [9], became another reason for the idea of anisotropy to remain strong in DES. A spherically symmetric model with a hypersurface was proposed by Lobo [10], in which the negative radial pressure, positive anisotropy parameter, and negative gravity profile are the features of DES. For the first time, he investigated the stability of this star. Ghezzi [11] introduced a configuration of the inner spacetime of DES, which in addition to dark energy, contained a neutron gas. Unlike Lobo's work [10] where the radial and transverse pressures were equal only at the center of the star, Ghezzi equated these two pressures inside the star, and considered them to be different only at the surface. He showed that the maximum mass of DES depends on the coupling parameter. Also, a non-singular stable model of DES was presented in which the radial pressure was proportional to the matter density [12]. On the other hand, a combination of baryonic matter and the phantom scalar field was a model that contained an exact solution for DES [13]. In this way, various models of DES were presented over time, most of them referring to the anisotropy parameter and stability of the star. In addition, other definable properties were also studied for it [14–17]. Of course, it was shown in Ref. [18] that the intervention of the phantom field can cause the instability of the star. The time dependence of Einstein's equations and the existence of a negative final pressure for a DES created a configuration to have no central singularity [19]. The radial oscillations of DES governed by the extended equation of state (EOS) of Chaplygin gas were measured by Panotopoulos et al. [20]. Assuming the presence of slow rotations in DES, measurements for an isotropic sample showed that the moment of

---

\* email address: a.bagheri@hafez.shirazu.ac.ir

† email address: ghbordbar@shirazu.ac.ir

‡ email address: eslampanah@umz.ac.ir

inertia of a rotating star is less than a non-rotating star [21]. Solving the Einstein-Maxwell field equations in a model of Finch-Skea spacetime [22] was done by Malaver [23]. He stated that the physical parameters of a DES behave well in the presence of electric charge. Recently, for two cases of isotropic and anisotropic DESs, Pretel [24] investigated other physical quantities such as the radial pulsations and tidal deformation.

Modified gravity can be important in the field of DES structure in two ways. First, in line with general relativity (GR), it can improve the results of modified gravity compared to GR without changing the concept of dark energy. For example, Malaver et al. [25] showed that the physical properties of a DES are maintained in Einstein-Gauss-Bonnet gravity. Also, by assuming the dependence of metric potentials on energy, Tudeschi et al. [26] demonstrated in addition to satisfying the characteristics of DES, the stability of a star near the surface depends on energy, and the results obtained in gravity's rainbow are improved compared to GR gravity. Secondly, the origin of late acceleration of the universe is not yet precisely known. In general, the concept of dark energy and the cosmological constant try to solve the problem based on the demand of GR.

However, persistent problems in cosmology have led to views of modified gravitation as an alternative to dark energy. One such theory is called massive gravity, which was first formulated by Pauli and Fierz [27]. The introduction of a spin-2 mass field in this theory, especially the assignment of mass to the graviton, became a turning point to justify the recent accelerated expansion at large distances without needing the dark energy. However, this linear theory had a fundamental flaw. In the massless limit of graviton, it does not satisfy GR. A non-linear method was an idea that Vainshtein [28] offered to remove this problem. But Boulware and Deser (BD) [29] showed that the existence of the ghost in this non-linear theory becomes another problematic factor. In order to solve this problem, there were many studies that have led to the formation of sub-branches in massive gravity. For example, the new massive gravity (NMG) in three dimensions [30]. In 2009 and 2010 in two studies [31, 32], it was shown that by using the graviton's mass and polynomial interaction terms involved in spacetime action, BD-ghost can be prevented. This is possible by introducing a reference metric. This method is known as dRGT massive gravity. Providing an exact static solution of the black hole in this gravity [33] allowed the study of compact objects in the presence of dRGT massive gravity to be strengthened. In particular, the presence of two additional terms in the massive metric coefficients compared to GR gravity can be a justification for dark matter and dark energy in massive gravity. It can be seen from this point of view that the massive graviton can play the role of cosmological constant in cosmic distances [34–37]. Also, the multi-gravity theory has tried to solve the BD-ghost problem in multi-dimensional spacetime for interacting spin-2 fields by applying the vielbein formulation [38]. In another interesting study, Hassan and Rosen showed that by using a dynamic reference metric instead of a static reference metric, the BD-ghost can be neglected in a non-linear bimetric theory for a massless spin-2 field [39]. A branch of dRGT massive gravity theory was proposed in 2013 by Vegh [40]. By applying holographic principles and a singular reference metric, he was able to establish a ghost-free theory. After the introduction of Vegh's model, many works were done in this field. Hendi et al., [41–46] studied the stability and thermodynamics of black holes by investigating the effect of massive parameters. Also, in Ref. [47], they investigated the physical quantities of the neutron star, including the maximum mass, using AV18 potential method. Eslam Panah and Liu [48] demonstrated that the maximum mass of a white dwarf in the presence of this gravity is greater than the Chandrasekhar limit. It was indicated that the end state of Hawking evaporation led to a black hole remnant in Vegh's massive gravity, which could help to ameliorate the information paradox [49]. Also, there was a correspondence between black hole solutions of conformal and Vegh's massive theories of gravity is found [50]. The remarkable point in Vegh's massive gravity is that the metric coefficients of spacetime do not have a term with the square of the distance  $r^2$ . In the sense that cosmological constant  $\Lambda$  can be defined for it separately. In addition, in the definition of a DES [7], we are dealing with dark energy that has a much greater density than the cosmological constant. Therefore, in the present study, we investigate the physical characteristics of this compact object by using Vegh's massive gravity and introducing dark energy in the form of fluid inside the inner spacetime.

In the last two decades, various observational and theoretical methods were introduced to constrain the range of graviton's mass. Among others, we can mention the observation of gravitational waves emitted by the merger of a binary system, which was carried out by the LIGO-Virgo collaboration. In this measurement, the range of graviton's mass in the GW170104 event was determined to be  $m_g < 7.7 \times 10^{-23} \text{eV}$  [51]. To learn about other methods, one can see Refs. [52, 53]. On the other side of the theory, the idea is raised that why should the mass of graviton be constant. Attributing variable mass dependent on the scalar field is the work that was done in response to this question by Huang et al., [54], which is known as Mass-varying massive gravity (MVMG). Following that, a number of additional studies have been conducted, including investigating the effect of the massive graviton in strong and weak gravitational environments. The authors [55] suggested that the mass of graviton near a black hole could be  $10^{23} \text{eV}$  orders of magnitude greater than that in the presence of weak gravitational fields. Also, in another study [56], these effects on neutron stars and white dwarfs were checked, which showed that the results agreed with the Ref. [55] reported an increase in the mass of graviton near the star.

In the present work, in order to compare the behavior of DES in the presence of massive gravitons with the observational results obtained so far, we use the observational measurement of the GW190814 event [57] and the

mass-radius relation for NS pulsars J1614-2230 [58], J0348+0432 [59], J0740+6620 [60] and J2215+5135 [61]. We also use the observational results of a binary system including the giant 2MASS J05215658+4359220 and a massive unseen companion [62].

In this paper, we follow the scheme of this study as follows: in Sec. II, we take a look at the background and relations of Vegh's massive gravity. Then, considering a spherical symmetric spacetime in Sec. III, we obtain the equations of motion and by using them, we introduce the TOV equation for the anisotropic distribution in Vegh's massive gravity. In this section and in the following, we present EOS and a model for the existence of anisotropy. In Sec. IV, by numerically solving the modified TOV equation, we obtain and analyze the properties of DES, such as maximum mass and its corresponding radius, radial pressure and transverse pressure, anisotropy parameter, surface redshift, etc. Finally, in Sec. V, we present a summary of the results obtained from this study.

## II. MASSIVE GRAVITY

In ghost free massive gravity, the action is given by [32]

$$I = \frac{c^4}{16\pi G} \int d^4x \sqrt{-g} [\mathcal{R} + m_g^2 \sum_i^4 c_i u_i(g, f)] + I_{matter}, \quad (1)$$

where  $c$  and  $G$  are the speed of light and the gravitational constant, respectively. Also,  $\mathcal{R}$  is the Ricci scalar and  $m_g$  refers to the graviton mass. In the second term on the right side of the action (potential term),  $c_i$  are constant coefficients that play the role of free parameters of action. Also  $u_i$  are introduced as symmetric polynomials of the eigenvalues of matrix  $K^a{}_b = \sqrt{g^{ac}f_{cb}}$ . Here  $g_{ab}$  is dynamical metric tensor and  $f_{ab}$  is called the reference metric. At the end of the above action,  $I_{matter}$  implies the action of matter.  $u_i$  are expressed in the following form

$$u_i = \sum_{y=1}^i (-1)^{y+1} \frac{(i-1)!}{(i-y)!} u_{i-y} [K^y], \quad (2)$$

where  $u_{i-y} = 1$ , when  $i = y$ . Note; in the above relations, the bracket marks indicate the traces in the form;  $[K] = K^a{}_a$  and  $[K^n] = (K^n)^a{}_a$ . Here we intend to specify the equations of motion in massive gravity, thus by varying the action with respect to metric tensor  $g_{ab}$ , and after doing some calculations, the equations are obtained as follows

$$G_{ab} + m_g^2 \chi_{ab} = \frac{8\pi G}{c^4} T_{ab}, \quad (3)$$

where  $G_{ab}$  is Einstein tensor,  $\chi_{ab}$  is called massive tensor and  $T_{ab}$  is stress-energy tensor. Note; in the following, we use geometrized units ( $c = G = 1$ ) for calculations. The massive tensor  $\chi_{ab}$  is extracted to form

$$\chi_{ab} = - \sum_{i=1}^{d-2} \frac{c_i}{2} \left[ u_i g_{ab} + \sum_{y=1}^i (-1)^y \frac{i!}{(i-y)!} u_{i-y} [K_{ab}^y] \right], \quad (4)$$

where  $d$  is related to the dimensions of spacetime. We work on 4-dimensional spacetime and so  $d = 4$ .

## III. EQUATIONS OF MOTION AND HYDROSTATIC EQUILIBRIUM EQUATIONS

We consider a spherically symmetric spacetime with metric signature  $(-, +, +, +)$

$$ds^2 = -e^{2\nu} dt^2 + e^{2\lambda} dr^2 + r^2 (d\theta^2 + \sin^2(\theta) d\phi^2), \quad (5)$$

where  $e^{2\nu}$  and  $e^{2\lambda}$  are the metric potentials. The spatial reference metric or spatial fiducial metric is a suitable option for the black hole solutions [40, 47, 48, 63]. Hence we suppose

$$f_{ab} = \text{diag} (0, 0, C^2, C^2 \sin^2 \theta), \quad (6)$$

where  $C$  is a positive constant. Using the line element Eq. (5) and reference metric Eq. (6), we can determine the tensor  $K^a{}_b$

$$K^a{}_b = \text{diag} \left( 0, 0, \frac{C}{r}, \frac{C}{r} \right), \quad (7)$$

and

$$\begin{aligned}
(K^2)^a{}_b &= \begin{bmatrix} 0 & 0 & 0 & 0 \\ 0 & 0 & 0 & 0 \\ 0 & 0 & \frac{C^2}{r^2} & 0 \\ 0 & 0 & 0 & \frac{C^2}{r^2} \end{bmatrix}, \\
(K^3)^a{}_b &= \begin{bmatrix} 0 & 0 & 0 & 0 \\ 0 & 0 & 0 & 0 \\ 0 & 0 & \frac{C^3}{r^3} & 0 \\ 0 & 0 & 0 & \frac{C^3}{r^3} \end{bmatrix}, \\
(K^4)^a{}_b &= \begin{bmatrix} 0 & 0 & 0 & 0 \\ 0 & 0 & 0 & 0 \\ 0 & 0 & \frac{C^4}{r^4} & 0 \\ 0 & 0 & 0 & \frac{C^4}{r^4} \end{bmatrix}, \tag{8}
\end{aligned}$$

and also

$$\begin{aligned}
[K] &= \frac{2C}{r}, \quad \& \quad [K^2] = \frac{2C^2}{r^2}, \\
[K^3] &= \frac{2C^3}{r^3}, \quad \& \quad [K^4] = \frac{2C^4}{r^4}. \tag{9}
\end{aligned}$$

Since we are working on four-dimensional spacetime, the only non-zero terms of  $u_i$  are  $u_1$  and  $u_2$  [46]. Therefore, using Eqs. (2), (7) and (9),  $u_i$  are obtained

$$\begin{aligned}
u_1 &= \frac{2C}{r}, \quad \& \quad u_2 = \frac{2C^2}{r^2}, \\
u_i &= 0, \quad \text{when } i > 2. \tag{10}
\end{aligned}$$

By putting Eq. (10) in Eq. (4), the elements of the massive tensor are determined

$$\begin{aligned}
\chi^1{}_1 &= -\frac{C(Cc_2 + c_1r)}{r^2}, \quad \& \quad \chi^3{}_3 = -\frac{c_1C}{2r}, \\
\chi^2{}_2 &= -\frac{C(Cc_2 + c_1r)}{r^2}, \quad \& \quad \chi^4{}_4 = -\frac{c_1C}{2r}. \tag{11}
\end{aligned}$$

We consider that the interior of the star is filled with an anisotropic fluid. The stress-energy tensor for an anisotropic distribution  $T_{ab}$ , is applied according to the following definition [64]

$$T_{ab} = [\rho(r) + p_t(r)]v_av_b + p_t(r)g_{ab} + [p_r(r) - p_t(r)]x_ax_b, \tag{12}$$

where  $\rho$ ,  $p_r$ , and  $p_t$  are the energy density, the radial pressure, and the transverse pressure, respectively. Also  $v_a$  refers to the four-velocity vector with  $v_av^a = -1$ , and  $x_a$  represents the unit spacelike vector with  $x_ax^a = 1$ . According to the metrics of the line element (5), the diagonal elements of the stress-energy tensor are obtained:

$$T_1^1 = -\rho(r), \quad \& \quad T_2^2 = p_r(r), \quad \& \quad T_3^3 = T_4^4 = p_t(r). \tag{13}$$

By substituting the above equations and the set of Eqs. (11) in Eq. (3), the equations of motion in massive gravity are obtained

$$\frac{2r\lambda'^{-2\lambda(r)} - e^{-2\lambda(r)} + 1 + m_g^2C(c_2C + c_1r)}{r^2} = 8\pi\rho(r), \tag{14}$$

$$\frac{2r\nu'^{-2\lambda(r)} + e^{-2\lambda(r)} - 1 - m_g^2C(c_2C + c_1r)}{r^2} = 8\pi p_r(r), \tag{15}$$

$$e^{-2\lambda(r)} \left[ \nu''(r) - \lambda'(r)\nu'(r) + \nu'^2(r) - \frac{\lambda'(r)}{r} + \frac{\nu'(r)}{r} \right] - \frac{c_1m_g^2C}{2r} = 8\pi p_t(r), \tag{16}$$

where the prime and double prime are representing the first and second derivatives with respect to  $r$ , respectively. Here consider the last term on the right side of the Eqs. (14) and (15), if we move the graviton mass terms to the other side of equality, we can see that the massive gravitons are similar to a fluid which has pressure and density. Another interesting point is that according to Eqs. (15) and (16), we realize that the pressure caused by gravitons is anisotropic. This anisotropic fluid can pattern the behavior of the dark matter halo on large scale [65].

The first equality of the equations of motion (14) leads us to the following relation

$$e^{-2\lambda(r)} = 1 - \frac{2m(r)}{r} + m_g^2 C \left( \frac{c_1 r}{2} + c_2 C \right), \quad (17)$$

and

$$m(r) = \int_0^r 4\pi r'^2 \rho(r') dr', \quad (18)$$

where  $m(r)$  shows the mass-energy function. Using the second equality (15), we obtain the gravity profile relation,

$$g(r) = \frac{d\nu(r)}{dr} = \frac{C c_1 m_g^2 r^2 + 16\pi p_r r^3 + 4m(r)}{2r (2C^2 c_2 m_g^2 r + C c_1 m_g^2 r^2 - 4m(r) + 2r)}. \quad (19)$$

The conservation condition must be satisfied. So, we have  $\nabla^a T_{ab} = 0$ . Now, by putting Eq. (19) in the conservation relation, and solving it in terms of the radial pressure gradient, the hydrostatic equilibrium equation in Vegh's massive gravity for an anisotropic distribution is obtained in the following form,

$$\frac{dp_r(r)}{dr} = \frac{[(4\pi r^3 p_r(r) + m(r)) + C c_1 m_g^2 r^2 / 4] (\rho(r) + p_r(r))}{-r (C c_1 m_g^2 r^2 / 2 - 2m(r) + r(m_g^2 c_2 C^2 + 1))} + \frac{2(p_t(r) - p_r(r))}{r}. \quad (20)$$

In the next step, we must introduce the EOS that can show the behavior of dark energy, and a model to describe the fluid anisotropy in order to solve the TOV equation. A suitable choice is generalized Chaplygin gas EOS  $p = -\frac{B}{\rho^\omega}$ , plus a linear term, which is written as follows [66, 67],

$$p_r = \hat{A}\rho - \frac{\hat{B}}{\rho^\omega}, \quad (21)$$

where  $\hat{A}$  is a positive dimensionless constant, and  $\hat{B}$  is a positive dimension constant in  $[L]^{-4}$  units and the parameter  $\omega$  is in the range  $(0, 1]$ . The first term is related to a barotropic fluid, and the second term refers to the generalized form of the Chaplygin gas EOS [68–70]. Such an EOS is an alternative to phantom and quintessence models in dark energy theory. We can consider the EOS (21) with  $\omega = 1$  in the following form for convenience in calculations, [20, 21, 71]

$$p_r = A^2 \rho - \frac{B^2}{\rho}. \quad (22)$$

In order to compare the results obtained from DES models with the extended Chaplygin EOS in GR [20, 21] and massive gravity (our suggestion), here we consider the constants  $A$  and  $B$  of the EOS as  $A = \sqrt{0.4}$  and  $B = 0.23 \times 10^{-3} km^{-2}$ . It should be noted that for the causality condition to be established at the star surface, the radial speed of sound  $V_{sr}$  must be satisfied in the range  $0 < V_{sr}^2(R) < 1$ . consequently,  $A^2 < 0.5$  [24]. In this way, the permissible range for choosing constant values of  $A$  is determined. By identifying the values of  $A$  and keeping the considerations of density and numerical solution,  $B$  can be selected.

The anisotropy parameter  $\Delta$  represents the difference between transverse pressure and radial pressure,  $p_t - p_r$ . The main cause of anisotropy in compact objects is the presence of densities greater than the nuclear density, which can be due to the presence of condensation [72], phase transition [73] or electromagnetic fields [74]. It is important that which model can be proposed to correctly describe the anisotropy behavior caused by the difference between radial and transverse pressure inside the star. Several models for anisotropy have been proposed in various studies [75–80]. The model that we extract in the present work is a nonlinear anisotropy that was first proposed by Bowers and Liang [75] in general form and is expressed as follows,

$$\Delta = p_t - p_r = \frac{\gamma(\rho + 3p_r)(\rho + p_r)r^n}{1 - \frac{2m}{r}}, \quad (23)$$

where the constant  $\gamma$  measures the degree of anisotropy, and the constant  $n$  is greater than 1. Since in a realistic model of compact objects  $(M/R)_{critical} > 0$ , the allowed range is  $\gamma \leq 2/3$ . In order to eliminate the anisotropy in the center of the star, we must consider  $n = 2$ . As a result, the final model of anisotropy parameter that we use in this study is defined as follows,

$$\Delta = \frac{\gamma(\rho + 3p_r)(\rho + p_r)r^2}{1 - \frac{2m}{r}}. \quad (24)$$

Therefore, our proposed model in this work for a dark energy star is introduced by extended Chaplygin gas Eq. (22) and the anisotropy parameter Eq. (24), which is formulated in the framework of massive gravity. For  $\gamma = 0$  and  $m_g = 0$ , the results describe an isotropic DES in GR that depends only on the proposed model for the EOS [20, 21].

#### IV. PROPERTIES OF DARK ENERGY STARS IN MASSIVE GRAVITY

##### A. Numerical Solutions

The star structure is determined by solving three coupled differential equations, Eqs. (18), (19), (20), and using the governing EOS (22) and anisotropy parameter (24). At the center of the star  $r = 0$ , the initial conditions are  $m(r = 0) = 0$  and  $\rho(r = 0) = \rho_c$ , where  $\rho_c$  is the central energy density. At the surface of the star, the radial pressure is negligible. Therefore the boundary conditions on the surface  $r = R$  are  $p_r(R) = 0$ ,  $m(r = R) = M$  and  $\nu(R) = \frac{1}{2} \ln \left( 1 - \frac{2M}{R} + m_g^2 C \left( \frac{c_1 R}{2} + c_2 C \right) \right)$ , where  $M$  is the total mass of DES. After integration from the center  $r = 0$  to the surface of the star, the radius  $R$  and mass  $M$  are obtained. Also, due to the dependence of  $M$  and  $R$  to  $\rho_c$  (or  $p_{r,c}$ ), by considering different values of central energy density (or central radial pressure), we will be able to determine the maximum mass for DES models. In the numerical solution, it is important to pay attention to the fact that the anisotropy parameter is zero in the center ( $\Delta(r = 0) = 0$ ), and the energy density on the surface is  $\rho_s = B/A$ . In addition, Eqs. (18) and (20) contain terms  $m_g^2 c_1$ ,  $m_g^2 c_2$ , and constant  $C$  that show the dependence of solution on the mass of graviton and the free parameters. With Ref. [47, 48, 81], here we consider the mass of graviton to be  $1.78 \times 10^{-65} g$ . The results obtained from the numerical solution are presented for the central density  $\rho_c = 1.34 \times 10^{15} g/cm^3$ , and the central pressure  $p_c = 4.33 \times 10^{15} dyn/cm^2$  in Tables. I-III.

TABLE I: The properties of dark energy star in massive gravity for  $C = 10^{-3}$ ,  $m_g^2 c_2 = -2 \times 10^{-2}$ ,  $\gamma = 0.1$ ,  $A = \sqrt{0.4}$  and  $B = 0.23 \times 10^{-3}$ .

$m_g^2 c_1$	$M_{max}(M_\odot)$	$R (km)$	$\sigma$	$z_s$
$3 \times 10^{-1}$	2.55	12.36	0.61	0.60
$3 \times 10^{-2}$	2.71	12.71	0.63	0.65
$3 \times 10^{-3}$	2.72	12.83	0.63	0.64
$3 \times 10^{-4}$	2.73	12.84	0.63	0.64
$-3 \times 10^{-1}$	2.95	13.31	0.66	0.71
$-3 \times 10^{-2}$	2.75	12.87	0.63	0.65
$-3 \times 10^{-3}$	2.73	12.84	0.63	0.64
$-3 \times 10^{-7}$	2.73	12.84	0.63	0.64

##### B. Pressure, density and anisotropy

According to the Eqs. (18), (20), (21), (22) and (24), and by using a numerical solution, the density, radial pressure, and anisotropy parameter versus the radius are plotted in the Figs. 1-3, respectively. Figs. 1 and 2 show that the density and radial pressure are a decreasing function of the radius, as it is expected. In both plots, it can be seen that the different values of  $C$ , and  $m_g^2 c_1$  affect the behavior of the density and radial pressure. It should be also noted that different values of  $m_g^2 c_2$  have no effect on changes in these quantities. According to the left panel of Fig. 3, it

TABLE II: The properties of dark energy star in massive gravity for  $m_g^2 c_1 = -3 \times 10^{-1}$ ,  $m_g^2 c_2 = -2 \times 10^{-2}$ ,  $\gamma = 0.1$ ,  $A = \sqrt{0.4}$  and  $B = 0.23 \times 10^{-3}$ .

$C$	$M_{max}(M_\odot)$	$R$ (km)	$\sigma$	$z_s$
$10^{-3}$	2.95	13.31	0.66	0.71
$10^{-4}$	2.75	12.87	0.63	0.65
$0.5 \times 10^{-4}$	2.74	12.85	0.63	0.64
$8 \times 10^{-5}$	2.74	12.86	0.63	0.65
$2 \times 10^{-5}$	2.73	12.84	0.63	0.64
$2 \times 10^{-6}$	2.73	12.84	0.63	0.64

TABLE III: The properties of dark energy star in massive gravity for  $C = 10^{-3}$ ,  $m_g^2 c_1 = -3 \times 10^{-1}$ ,  $\gamma = 0.1$ ,  $A = \sqrt{0.4}$  and  $B = 0.23 \times 10^{-3}$ .

$m_g^2 c_2$	$M_{max}(M_\odot)$	$R$ (km)	$\sigma$	$z_s$
$-2 \times 10^{-4}$	2.95	13.31	0.66	0.71
$-3 \times 10^{-3}$	2.95	13.31	0.66	0.71
$-4 \times 10^{-2}$	2.95	13.31	0.66	0.71
$-5 \times 10^{-1}$	2.95	13.31	0.66	0.71
$-7 \times 10^{-1}$	2.95	13.31	0.66	0.71
$-9 \times 10^{-1}$	2.95	13.31	0.66	0.71

can be seen that the anisotropy parameter  $\Delta$  is also sensitive to the parameter  $C$ , and increases by its increasing. Therefore, the massive graviton and the dependence of its behavior on free parameters can affect the results obtained from density, pressure, and anisotropy. The factor  $\Delta/r$  creates a positive force in the outward direction of the star. This is an important feature of a DES, because it ensures the stability of the star. It is interesting to examine the

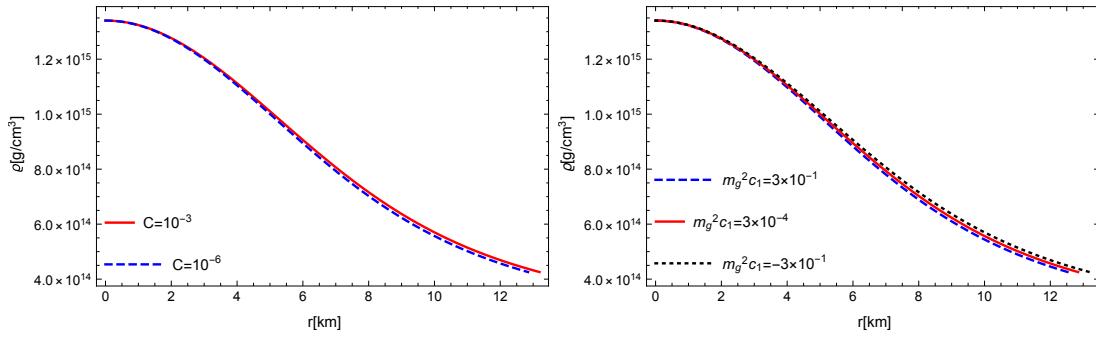


FIG. 1: Density  $\rho$  vs radius  $r$  for different  $C$  (left panel) and for different  $m_g^2 c_1$  (right panel) with  $m_g^2 c_2 = -2 \times 10^{-2}$ ,  $\gamma = 0.1$ ,  $A = \sqrt{0.4}$  and  $B = 0.2 \times 10^{-3}$ .

change in the behavior of the anisotropy parameter by changing the value of parameter  $\gamma$  versus radius. In the right panel of Fig. 3, the  $\Delta$  diagram is drawn in terms of different values of  $\gamma$ . It can be seen that with the increasing in the amount of  $\gamma$ , the amount of anisotropy also increases. This means that the force caused by it also increases towards the outside of the star, and the star will be more resistant to gravitational collapse.



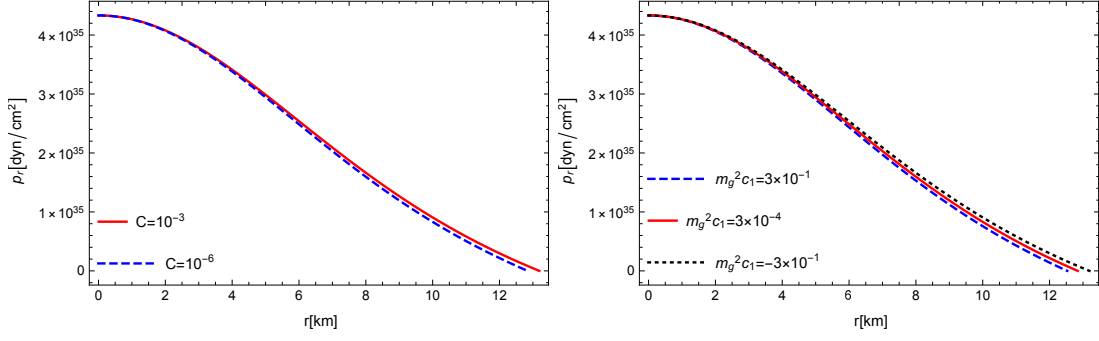


FIG. 2: Radial pressure  $p_r$  vs radius  $r$  for different  $C$  (left panel) and for different  $m_g^2 c_1$  (right panel) with  $m_g^2 c_2 = -2 \times 10^{-2}$ ,  $\gamma = 0.1$ ,  $A = \sqrt{0.4}$  and  $B = 0.2 \times 10^{-3}$ .

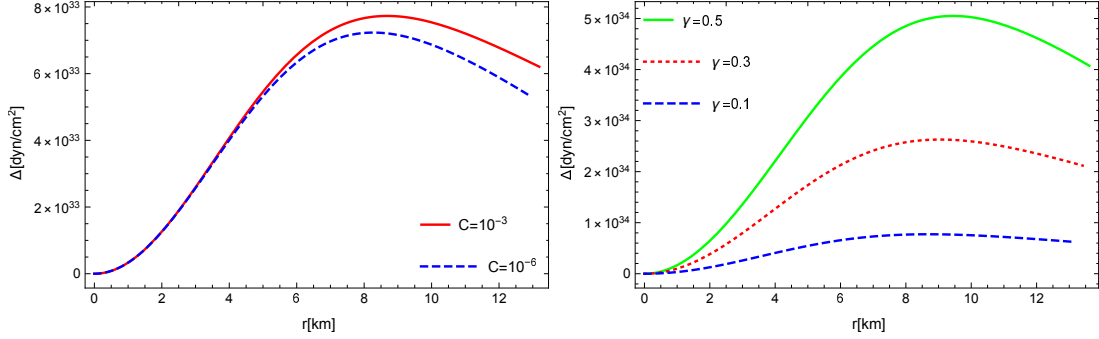


FIG. 3: Anisotropy parameter  $\Delta$  vs radius  $r$  for different  $C$  and  $\gamma = 0.1$  (left panel) and for  $C = 10^{-3}$ ,  $m_g^2 c_1 = -3 \times 10^{-1}$ ,  $m_g^2 c_2 = -2 \times 10^{-2}$ ,  $A = \sqrt{0.4}$ ,  $B = 0.2 \times 10^{-3}$  and different  $\gamma$  (right panel).

### C. Maximum mass, compactness and surface redshift

Studying the structure of DESs in detail is difficult, because the basic nature of dark energy is still unknown. Also, various models for the inner region of this star have been proposed so far. Depending on what the dark energy candidate is, and its other constituents, we will be able to estimate its mass function and maximum mass. In two studies [11, 17], it was shown that the maximum mass of a DES is about  $2M_\odot$  and  $2.5M_\odot$ , respectively. For the special case of extended Chaplygin EOS, Panotopoulos et al. [20, 21] showed that these maxima depend on the constants of the EOS in the absence of anisotropy, and the maximum mass belongs to the category of heavy stars ( $M \sim 2M_\odot$ ). Also, in a recent study [24], it was shown that in the presence of anisotropy, and by assuming different values for constants of the equation of state, the maximum mass can exceed the range of  $2.5M_\odot$  in general relativity.

Fig. 4 demonstrates the mass-radius relation and central mass-density relation for different models (isotropic-anisotropic configuration in the framework of GR and isotropic and anisotropic configuration in the framework of massive gravity) of DES. The DES model we presented here evokes an isotropic (anisotropic) compact object in the GR with  $m_g = 0$  and  $\gamma = 0$  or  $\gamma \neq 0$ . For non-zero values of  $m_g$  and  $\gamma = 0$  or  $\gamma \neq 0$ , a modified isotropic model (anisotropic model) of DES is created in massive gravity. The gravitational mass versus radius diagrams in massive gravity (MG) for a series of central densities and for different values of  $C$ ,  $m_g^2 c_1$ ,  $m_g^2 c_2$  and  $\gamma$  are drawn in Fig. 5. The maximum mass and radius of this model of DES increase with increasing  $C$ , and reach the final limit for  $C = 10^{-3}$ . On the other hand, as  $C$  decreases, the maxima decrease and eventually reach the limit of the anisotropic model of GR ( $M = 2.73M_\odot$ , and  $R = 12.84\text{km}$ ) (see the up left panel in Fig. 5). For the positive values assigned to  $m_g^2 c_1$  with a reduction of the order of  $10^{-1}$ , the maximum mass and radius have an increasing trend. But as the negative values of  $m_g^2 c_1$  increase, the maxima are reduced (see the up right panel in Fig. 5). As it is clear from the results in the down left panel of Fig. 5, by considering different values of  $m_g^2 c_2$ , the maximum mass and radius do not change, and remain fixed, but compared to the case  $m_g = 0$  (GR), an increasing in maximum mass and radius is observed. In fact, the obtained results depend on the choice of other massive free parameters. Also, we can see that as the anisotropy parameter  $\gamma$  increases, the maximum mass also increases in massive gravity (see the down right panel in



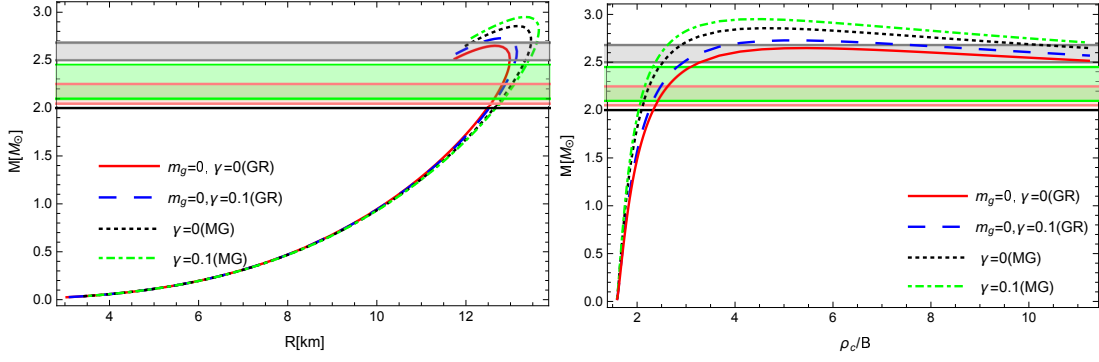


FIG. 4: Mass-radius plot (left panel) and mass-central density plot (right panel) for DES with  $A = \sqrt{0.4}$  and  $B = 0.2 \times 10^{-3}$ . At  $2M_\odot$ , the black horizontal line indicates the mass limit of the massive NS pulsars (J1614-2230 and J0348+0432). The wide pink and green bars display the observational mass data of NS pulsars J0740+6620 and J2215+5135, respectively. Observational data from event GW190814 are applied in the gray area.

Fig. 5). Note that according to Tables. I-III and Fig. 5, the maximum mass in massive gravity goes up to the interval  $2.95M_\odot - 3.5M_\odot$ , which can be located within the mass gap range,  $2.5M_\odot - 5M_\odot$ . This result, in addition to covering the observational constraints, can be a candidate for the massive unseen companion in the binary system 2MASS J05215658+4359220 whose mass range is estimated to be  $3.3_{-0.7}^{+2.8}M_\odot$  [62], and remnant mass of GW190425 [82, 83].

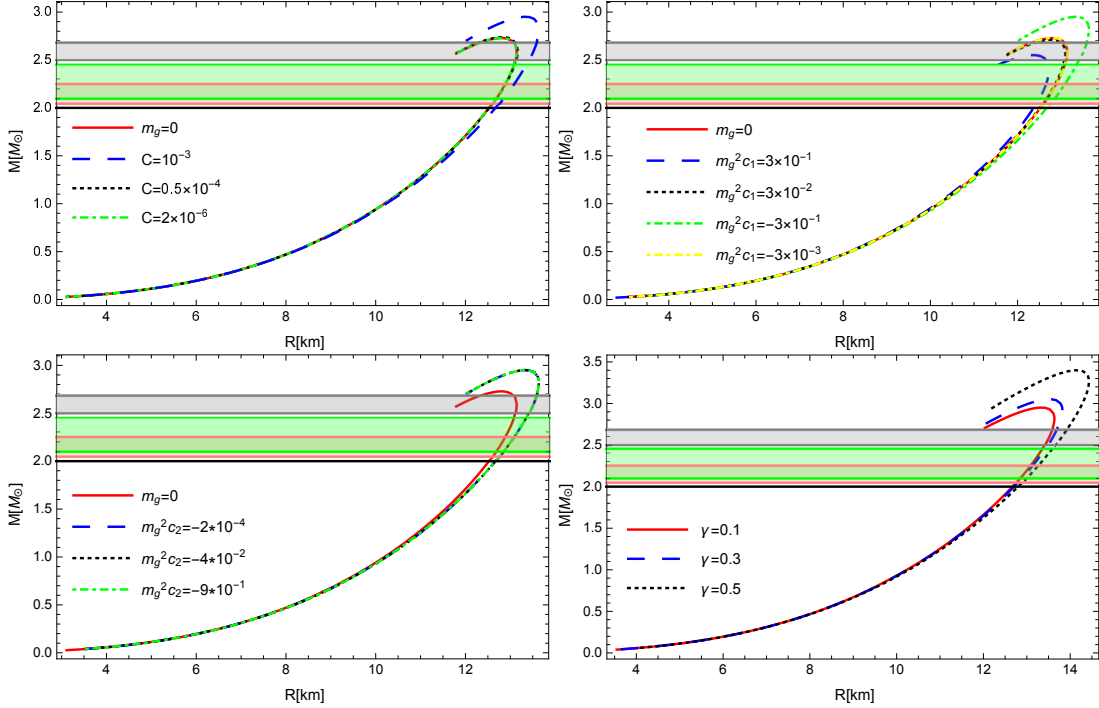


FIG. 5: Gravitational mass vs radius in massive gravity for: Different  $C$  with  $m_g^2 c_1 = -3 \times 10^{-1}$ ,  $m_g^2 c_2 = -2 \times 10^{-2}$  and  $\gamma = 0.1$  (up left panel). Different  $m_g^2 c_1$  with  $C = 10^{-3}$ ,  $m_g^2 c_2 = -2 \times 10^{-2}$  and  $\gamma = 0.1$  (up right panel).

Different  $m_g^2 c_2$  with  $C = 10^{-3}$ ,  $m_g^2 c_1 = -3 \times 10^{-1}$  and  $\gamma = 0.1$  (down left panel). Different  $\gamma$  and  $C = 10^{-3}$ ,  $m_g^2 c_1 = -3 \times 10^{-1}$ ,  $m_g^2 c_2 = -2 \times 10^{-2}$  (down right panel). The descriptions of colored areas are given in the caption of Fig. (4).

To calculate compactness  $\sigma = R_{sch}/R$ , one needs to obtain the Schwarzschild radius  $R_{sch}$  in the massive gravity. The compactness can induce the power of gravity. By equalizing the Eq. (17) with zero, after some calculations, the

modified Schwarzschild radius is determined as follows [47, 48],

$$R_{sch} = \frac{-(1 + C^2 c_2 m_g^2) + \sqrt{(1 + C^2 c_2 m_g^2)^2 + 4C c_1 m_g^2 M}}{C m_g^2 c_1}. \quad (25)$$

In general, the gravitational redshift is related to the metric potential,  $1 + z = e^{\lambda(r)}$ , which the surface redshift  $z_s$  can be written in the following form using Eq. (17) in massive gravity [47],

$$1 + z_s = \frac{1}{\sqrt{1 - \frac{2M}{R} + m_g^2 C \left( \frac{c_1 R}{2} + c_2 C \right)}}. \quad (26)$$

For different values of  $m_g^2 c_1$ ,  $m_g^2 c_2$  and  $C$ , the obtained results are shown in Tables. I-III. By changing the values of  $m_g^2 c_2$ , the compactness  $\sigma$  and surface redshift  $z_s$  do not change, and remain the same for all values (see Table. III). The quantities  $\sigma$  and  $z_s$  decrease by decreasing the values of  $C$  (see Table. II). By decreasing the positive and negative values assigned to  $m_g^2 c_1$ , the quantities  $\sigma$  and  $z_s$  increase slightly (refer Table. I).

#### D. ENERGY CONDITION

In order to have a standard stellar model, in addition to other acceptable properties, the energy conditions must be satisfied [84, 85]. For our proposed model for a DES discussed at the end of Sec. III, using the energy density  $\rho$ , radial pressure  $p_r$  and transverse pressure  $p_t$ , we examine the energy conditions such as the null energy condition (NEC), weak energy condition (WEC), strong energy condition (SEC), and dominant energy condition (DEC) for DES. The requirements of each energy condition can be summarized as,

$$\begin{aligned} NEC &\rightarrow \begin{cases} \rho + p_r \geq 0 \\ \rho + p_t \geq 0 \end{cases}, \quad \& \quad WEC \rightarrow \begin{cases} \rho \geq 0 \\ \rho + p_r \geq 0 \\ \rho + p_t \geq 0 \end{cases}, \\ SEC &\rightarrow \begin{cases} \rho + p_r + 2p_t \geq 0 \\ \rho + p_t \geq 0 \end{cases}, \quad \& \quad DEC \rightarrow \begin{cases} |\rho| \geq |p_r| \\ |\rho| \geq |p_t| \end{cases}, \end{aligned} \quad (27)$$

Our results are given in Table. IV. As it is shown in Table. IV, the energy conditions are satisfied in inner DES. Although one of the characteristics of dark energy is the defect of the SEC condition ( $\rho + p_r + 2p_t < 0$ ), however, the presence of barotropic fluid makes the fluid to behave similar to a normal matter in terms of energy conditions. It should be noted that the investigation of these conditions in the presence of gravitons with non-zero mass does not have the different results with those in the case of gravitons with zero mass (general relativity).

TABLE IV: Energy conditions of DES in massive gravity for  $C = 10^{-3}$ ,  $m_g^2 c_1 = -3 \times 10^{-1}$ ,  $m_g^2 c_2 = -2 \times 10^{-2}$ ,  $A = \sqrt{0.4}$ ,  $\gamma = 0.1$  and  $B = 0.23 \times 10^{-3}$ .

(NEC)	(WEC)	(SEC)	(DEC)
✓	✓	✓	✓

#### E. EQUILIBRIUM AND STABILITY

To check the stability of compact objects, several theoretical methods have been stated, which can be referred to as stability tests. Here we follow some cases.

### 1. TOV equation

The structure of the star maintains its hydrostatic balance, if the sum of hydrostatic, gravitational, and anisotropic forces in the modified TOV equation becomes zero [14, 17]. Therefore, the following relation must hold,

$$F_h + F_g + F_a = 0, \quad (28)$$

where  $F_h$ ,  $F_g$ , and  $F_a$  are hydrostatic, gravitational and anisotropic forces, respectively. They define as,

$$F_h = -\frac{dp_r}{dr}, \quad (29)$$

$$F_g = -\frac{\nu'(\rho + p_r)}{2}, \quad (30)$$

$$F_a = \frac{2(p_t - p_r)}{r}, \quad (31)$$

According to Eqs. (19), (20), and (24), the sum of forces can be obtained. Fig. 6 shows all forces and also their sum. As can be seen, the hydrostatic equilibrium is also established in massive gravity.

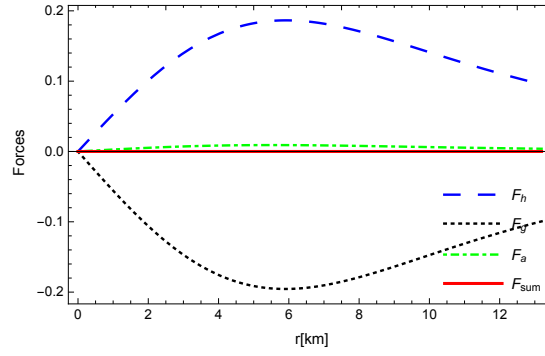


FIG. 6: Forces vs radius for  $C = 10^{-3}$ ,  $m_g^2 c_1 = -3 \times 10^{-1}$ ,  $m_g^2 c_2 = -2 \times 10^{-2}$ ,  $A = \sqrt{0.4}$ ,  $B = 0.2 \times 10^{-3}$  and  $\gamma = 0.1$ .

### 2. Causality

The condition of causality holds, if the speed of sound  $V_s$  obeys the relation  $0 \leq V_s^2 = \frac{dp}{d\rho} \leq 1$  [86]. For an anisotropic configuration, two quantities, the square of the radial speed of sound  $V_{sr}^2$  and the square of the transverse speed of sound  $V_{st}^2$ , can be measured as follows,

$$V_{sr}^2 = \frac{dp_r}{d\rho}, \quad (32)$$

$$V_{st}^2 = \frac{dp_t}{d\rho}. \quad (33)$$

Here, the speed of sound is obtained numerically, and the results are plotted in Figs. 7 and 8. It can be clearly seen that for different values of massive free parameters, two conditions  $0 \leq V_{sr}^2 \leq 1$  and  $0 \leq V_{st}^2 \leq 1$  are satisfied. Note that unlike what happens for the speed of sound inside the isotropic stars, here in the presence of an anisotropic configuration, the speed of sound can have an increasing trend. By reducing the massive parameter  $C$ , the speed of sound decreases. Also, the lowest value of  $V_{sr, st}$  corresponds to negative values of  $m_g^2 c_1$ . It is interesting to consider what consequences these local anisotropies can create in the star. Herrera [86] showed that in the presence of local anisotropies, a phenomenon called cracking occurs. Based on this idea, potentially stable regions  $-1 < V_{st}^2 - V_{sr}^2 < 0$  and potentially unstable regions  $0 < V_{st}^2 - V_{sr}^2 < 1$  are distorted according to speeds [87]. According to the Fig. 9, it is deduced that for non-zero values of  $\gamma$ , this anisotropic model Eq. (24) of DES is potentially unstable. This instability is caused by the presence of anisotropy in this configuration.

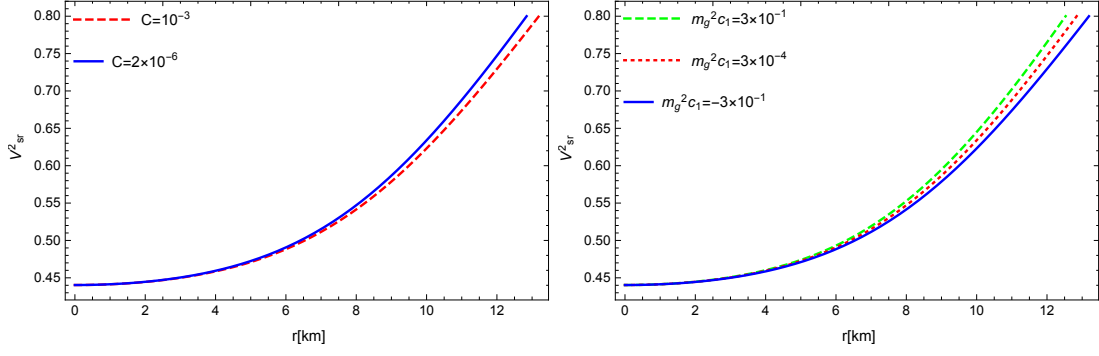


FIG. 7: Square of radial speed of sound  $V_{sr}^2$  in massive gravity for different  $C$  (left panel) and for different  $m_g^2 c_1$  (right panel) for DES with  $A = \sqrt{0.4}$ ,  $B = 0.2 \times 10^{-3}$ .

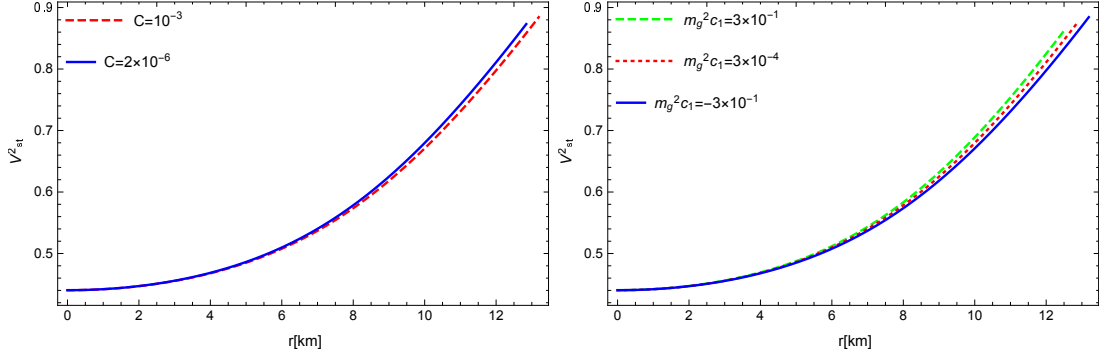


FIG. 8: Square of transverse speed of sound  $V_{st}^2$  in massive gravity for different  $C$  (left panel) and for different  $m_g^2 c_1$  (right panel) for DES with  $A = \sqrt{0.4}$ ,  $B = 0.2 \times 10^{-3}$  and  $\gamma = 0.1$ .

### 3. Adiabatic index

The adiabatic index can determine the stiffness of EOS for a specific density. It is also a suitable quantity to check the stability of star against the radial perturbations. According to some studies [88–90], a spherical configuration is stable if its adiabatic index be  $\Gamma = \left(1 + \frac{\rho}{p_r}\right) V_{sr}^2$ . The behavior of the adiabatic index is plotted in Fig. 10. It is clear that anywhere inside the DES, it has a value greater than  $4/3$ . Therefore, it can be stated that the configuration of the star is dynamically stable in massive gravity with  $\gamma = 0$  (isotropic), different values of  $C$  and  $m_g^2 c_1$ . But in the case of local anisotropy within the star, it was suggested to make corrections on the condition of adiabatic stability,

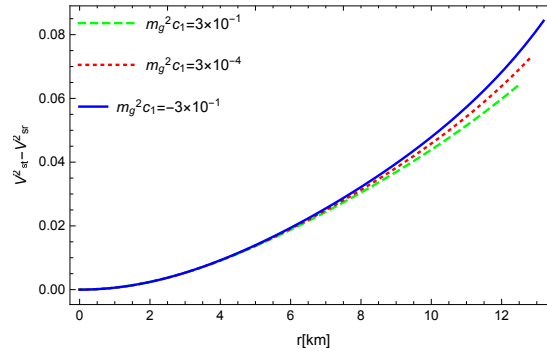


FIG. 9: Difference  $V_{st}^2 - V_{sr}^2$  for  $C = 10^{-3}$ ,  $m_g^2 c_2 = -2 \times 10^{-2}$ ,  $A = \sqrt{0.4}$ ,  $B = 0.2 \times 10^{-3}$ ,  $\gamma = 0.1$  and different  $m_g^2 c_1$ .

although the relativistic corrections make the increasing for the instability [90, 91]. Therefore, we will try another method in the following.

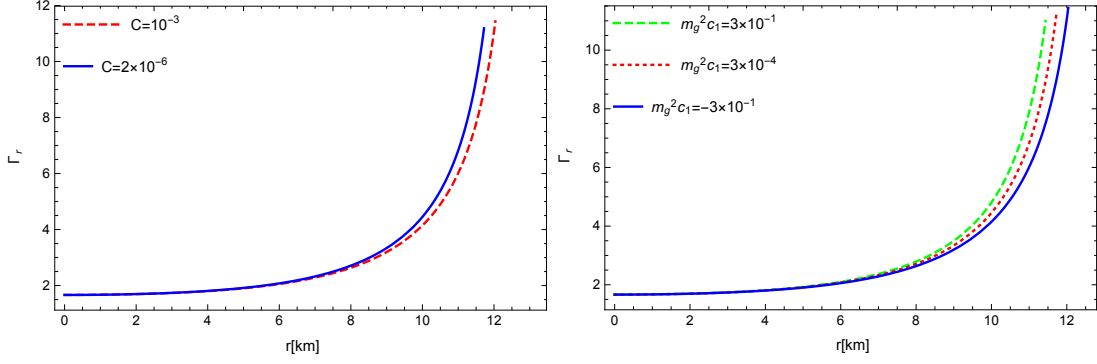


FIG. 10: Adiabatic index  $\Gamma$  in massive gravity for different  $C$  (left panel) and for different  $m_g^2 c_1$  (right panel) for DES with  $A = \sqrt{0.4}$  and  $B = 0.2 \times 10^{-3}$ .

#### 4. Harrison-Zeldovich-Novikov condition

Another example of the stability conditions of compact objects is known as Harrison-Zeldovich-Novikov condition [92, 93], which states that there are stable regions where condition  $dM/d\rho_c > 0$  is valid. In the right panel of Fig. 4, the maximum mass diagram versus central density  $\rho_c$  shows that the criterion  $dM/d\rho_c > 0$  is satisfied for the areas on the left side of the maximum point of the curves. So DES is stable up to this point with  $\rho_{crit}$ . As soon as we move from this density to higher densities (right side of the curves),  $dM/d\rho_c$  becomes negative, which indicates dynamical instability, and the star becomes capable of collapsing into a black hole.

In general, it can be pointed out that the existence of instability in the structure of compact objects can be caused by the two factors of EOS and anisotropy. Of course, which model is better for these two factors is not completely clear because, for our chosen model, the main nature of dark energy is not yet known.

## V. CONCLUSIONS

In this research, considering the massive graviton, we obtained the hydrostatic equilibrium equation in Vegh's massive gravity. For the extended Chaplygin gas EOS and a nonlinear model of anisotropy, the anisotropic modified TOV equation was solved numerically. After performing the numerical solution for the fixed coefficients of the EOS  $A$  and  $B$ , we obtained the density, radial pressure, and the anisotropy parameter depending on the mass of graviton  $m_g$ . We also showed that with an increasing degree of anisotropy, the anisotropy parameter ( $\gamma$ ) increased. By increasing it up to a certain limit, the maximum mass and radius increase. The force created by the presence of anisotropy is a factor preventing gravitational collapse. We showed that the obtained results from the numerical solution are sensitive to the variation of the values of massive free parameters  $m_g^2 c_1$ ,  $m_g^2 c_2$  and constant  $C$ . We saw that with the increase of parameter  $C$ , the maximum mass and radius are increased. Increasing the negative values of  $m_g^2 c_1$  results a decrease in the maximum mass and radius. It was also found that the changes in values of  $m_g^2 c_2$  has no effect on the maxima. We indicated that two important factors, the massive gravitons and anisotropy can improve the obtained results compared with the mass-radius constraint from the observational events. We also demonstrated that in the isotropic model, massive gravitons alone have the ability to increase the maximum mass-radius. Our proposed model for DES not only can be a candidate for mystery object from the gravitational-wave signal of GW190814, but also able to include mass values located in the lower mass gap range,  $2.5M_\odot - 5M_\odot$  [62, 94]. It was found that the compactness and the surface redshift of the DES does not change by variations  $m_g^2 c_2$ , and by decreasing the value of  $C$ , both decrease. Also, the highest value for the compactness and the surface redshift is related to the negative value of  $m_g^2 c_1$ , and the lowest value is obtained for the positive value of  $m_g^2 c_1$ . In order to investigate the stability of the DES structure, we used several different methods. We showed that the causality condition holds for the anisotropic configuration, but this model is potentially unstable. On the other hand, the star is dynamically stable for central densities lower than the critical density, and for densities higher than  $\rho_{crit}$ , it becomes unstable, and it is possible to

become a black hole. In summary, DES is important in the framework of massive gravity, because the role of massive gravitons in this method makes the proposed model closer to the observational results.

### Acknowledgments

A. Bagheri Tudesghi and G. H. Bordbar wish to thank Shiraz University research council. B. Eslam Panah thanks the University of Mazandaran. The University of Mazandaran has supported the work of B. Eslam Panah by title "Evolution of the masses of celestial compact objects in various gravity".

- 
- [1] R. R. Caldwell, R. Dave, and P. J. Steinhardt, Phys. Rev. Lett. 80 (1998) 1582.
  - [2] R. R. Caldwell, Phys. Lett. B 545 (2002) 23.
  - [3] A. Kamenshchik, U. Moschella, and V. Pasquier, Phys. Lett. B 511 (2001) 265.
  - [4] S. Coleman, and F. De Luccia, Phys. Rev. D 21 (1980) 3305.
  - [5] I. Dymnikova, Gen. Rel. Grav. 24 (1992) 235.
  - [6] P. O. Mazur, and E. Mottola, Proc. Nat. Acad. Sci. 101 (2004) 9545.
  - [7] G. Chapline, "Dark Energy Stars", [arXiv:astro-ph/0503200], 2005.
  - [8] G. Chapline, and J. Barbieri, Int. J. Mod. Phys. D 23 (2014) 1450025.
  - [9] C. Cattoen, T. Faber, and M. Visser, Class. Quantum Grav. 22 (2005) 4189.
  - [10] F. S. Lobo, Class. Quantum Grav. 23 (2006) 1525.
  - [11] C. R. Ghezzi, Astrophys. Space Sci. 333 (2011) 437.
  - [12] F. Rahaman, R. Maulick, A. K. Yadav, S. Ray, and R. Sharma, Gen. Rel. Grav. 44 (2012) 107.
  - [13] S. S. Yazadjiev, Phys. Rev. D 83 (2011) 127501.
  - [14] P. Bhar, and F. Rahaman, Eur. Phys. J. C 75 (2015) 1.
  - [15] P. Bhar, T. Manna, F. Rahaman, and A. Banerjee, Can. J. Phys. 96 (2018) 594.
  - [16] A. Banerjee, M. Jasim, and A. Pradhan, Mod. Phys. Lett. A 35 (2020) 2050071.
  - [17] P. Bhar, Phys. Dark Universe. 34 (2021) 100879.
  - [18] M. F. A. Ranga Sakti, and A. Sulaksono, Phys. Rev. D 103 (2021) 084042.
  - [19] P. Beltracchi, and P. Gondolo, Phys. Rev. D 99 (2019) 044037.
  - [20] G. Panotopoulos, A. Rincón, and I. Lopes, Eur. Phys. J. Plus. 135 (2020) 1.
  - [21] G. Panotopoulos, A. Rincón, and I. Lopes, Phys. Dark Universe. 34 (2021) 100885.
  - [22] M. R. Finch, and J. E. Skea, Class. Quantum Grav. 6 (1989), 467.
  - [23] M. Malaver, "Charged Dark Energy Stars in a Finch-Skea Spacetime", [arXiv:2206.13943], 2022.
  - [24] J. M. Pretel, Eur. Phys. J. C 83 (2023) 26.
  - [25] M. Malaver, et al., "A theoretical model of Dark Energy Stars in Einstein-Gauss-Bonnet Gravity", [arXiv:2106.09520], 2021.
  - [26] A. Bagheri Tudesghi, G. H. Bordbar, and B. Eslam Panah, Phys. Lett. B 835 (2022) 137523.
  - [27] M. Fierz, and W. E. Pauli, Proc. Roy. Soc. Lond. A 173 (1939) 211.
  - [28] A. I. Vainshtein, Phys. Lett. B 39 (1972) 393.
  - [29] D. G. Boulware, and S. Deser, Phys. Rev. D 6 (1972) 3368.
  - [30] E. A. Bergshoeff, O. Hohm, and P. K. Townsend, Phys. Rev. Lett. 102 (2009) 201301.
  - [31] C. de Rham, and G. Gabadadze, Phys. Rev. D 82 (2010) 044020.
  - [32] C. de Rham, G. Gabadadze, and A. J. Tolley, Phys. Rev. Lett. 106 (2011) 231101.
  - [33] S. G. Ghosh, L. Tannukij, and P. Wongjun, Eur. Phys. J. C 76 (2016) 1.
  - [34] A. De Felice, A. E. Gumrukcuoglu, C. Lin, and S. Mukohyama, Class. Quantum Grav. 30 (2013) 184004.
  - [35] D. Comelli, M. Crisostomi, F. Nesti, and L. Pilo, J. High Energy Phys. 3 (2012) 1.
  - [36] D. Langlois, and A. Naruko, Class. Quantum Grav. 29 (2012) 202001.
  - [37] T. Kobayashi, M. Siino, M. Yamaguchi, and D. Yoshida, Phys. Rev. D 86 (2012) 061505.
  - [38] K. Hinterbichler, and R. A. Rosen, J. High Energy Phys. 7 (2012) 1.
  - [39] S. F. Hassan, and R. A. Rosen, J. High Energy Phys. 2 (2012) 1.
  - [40] D. Vegh, "Holography without translational symmetry", [arXiv:1301.0537], 2013.
  - [41] S. H. Hendi, B. Eslam Panah, and S. Panahiyan, J. High Energy Phys. 11 (2015) 157.
  - [42] S. H. Hendi, S. Panahiyan, and B. Eslam Panah, J. High Energy Phys. 01 (2016) 129.
  - [43] S. H. Hendi, S. Panahiyan, B. Eslam Panah, and M. Momennia, Annalen der Physik. 528 (2016) 819.
  - [44] S. H. Hendi, B. Eslam Panah, and S. Panahiyan, Class. Quantum Grav. 33 (2016) 235007.
  - [45] S. H. Hendi, B. Eslam Panah, and S. Panahiyan, J. High Energy Phys. 05 (2016) 029.
  - [46] S. H. Hendi, R. B. Mann, S. Panahiyan, and B. Eslam Panah, Phys. Rev. D 95 (2017) 021501(R).
  - [47] S. H. Hendi, G. H. Bordbar, B. Eslam Panah, and S. Panahiyan, J. Cosm. Astropart. Phys. 07 (2017) 004.
  - [48] B. Eslam Panah, and H. L. Liu, Phys. Rev. D 99 (2019) 104074.
  - [49] B. Eslam Panah, S. H. Hendi, and Y. C. Ong, Phys. Dark Universe. 27 (2020) 100452.

- [50] B. Eslam Panah, and S. H. Hendi, *Europhys. Lett.* 125 (2019) 60006.
- [51] L. I. G. O. Scientific, V. Collaboration, and B. P. Abbott, *Phys. Rev. Lett.* 121 (2018) 129901.
- [52] A. S. Goldhaber, and M. M. Nieto, *Rev. Mod. Phys.* 82 (2010) 939.
- [53] E. Berti, J. Gair, and A. Sesana, *Phys. Rev. D* 84 (2011) 101501.
- [54] Q. G. Huang, Y. S. Piao, and S. Y. Zhou, *Phys. Rev. D* 86 (2012) 124014.
- [55] J. Zhang, and S. Y. Zhou, *Phys. Rev. D* 97 (2018) 081501.
- [56] X. Sun, and S. Y. Zhou, *Phys. Rev. D* 101 (2020) 044060.
- [57] R. Abbott et al., *Astrophys. J. Lett.* 896 (2020) L44.
- [58] P. Demorest, T. Pennucci, S. Ransom, M. Roberts, and J. Hessels, *Nature*. 467 (2010) 1081.
- [59] J. Antoniadis et al., *Science* 340 (2013) 1233232.
- [60] H. T. Cromartie et al., *Nat. Astronomy*. 4 (2019) 72.
- [61] M. Linares, T. Shahbaz, and J. Casares, *Astrophys. J.* 859 (2018) 54.
- [62] T. A. Thompson et al., *Science* 366 (2019) 637.
- [63] R. G. Cai, Y. P. Hu, Q. Y. Pan, and Y. L. Zhang, *Phys. Rev. D* 91 (2015) 024032.
- [64] S. S. Bayin, *Astrophys. J.* 303 (1986) 101.
- [65] S. Panpanich, and P. Burikham, *Phys. Rev. D* 98 (2018) 064008.
- [66] U. Debnath, A. Banerjee, and S. Chakraborty, *Class. Quantum Grav.* 21 (2004) 5609.
- [67] B. Pourhassan, *Int. J. Mod. Phys. D* 22 (2013) 1350061.
- [68] M. C. Bento, O. Bertolami, and A. A. Sen, *Phys. Rev. D* 66 (2002) 043507.
- [69] V. Gorini, A. Kamenshchik, and U. Moschella, *Phys. Rev. D* 67 (2003) 063509.
- [70] Y. D. Xu, Z. G. Huang, and X. H. Zhai, *Astrophys. Space Sci.* 339 (2012) 31.
- [71] F. Tello-Ortiz, M. Malaver, Á. Rincón, and Y. Gomez-Leyton, *Eur. Phys. J. C* 80 (2020) 371.
- [72] J. B. Hartle, R. F. Sawyer, and D. J. Scalapino, *Astrophys. J.* 199 (1975) 471.
- [73] A. I. Sokolov, *J. Exp. Theor. Phys.* 52 (1980) 575.
- [74] V. V. Usov, *Phys. Rev. D* 70 (2004) 067301.
- [75] R. L. Bowers, and E. P. T. Liang, *Astrophys. J.* 188 (1974) 657.
- [76] M. Cosenza, L. Herrera, M. Esculpi, and L. Witten, *J. Math. Phys.* 22 (1981) 118.
- [77] D. Horvat, S. Ilić, and A. Marunović, *Class. Quantum Grav.* 28 (2010) 025009.
- [78] D. D. Doneva, and S. S. Yazadjiev, *Phys. Rev. D* 85 (2012) 124023.
- [79] L. Herrera, and W. Barreto, *Phys. Rev. D* 88 (2013) 084022.
- [80] G. Raposo, P. Pani, M. Bezares, C. Palenzuela, and V. Cardoso, *Phys. Rev. D* 99 (2019) 104072.
- [81] A. F. Ali, and S. Das, *Int. J. Mod. Phys. D* 25 (2016) 1644001.
- [82] B. P. Abbott, et al., *Astrophys. J. Lett.* 892 (2020) L3.
- [83] J. Sedaghat, et al., *Phys. Lett. B* 833 (2022) 137388.
- [84] J. Ponce de Leon, *Gen. Rel. Grav.* 25 (1993) 1123.
- [85] M. Visser, "*Lorentzian Wormholes. From Einstein to Hawking*". Woodbury, 1995.
- [86] L. Herrera, *Phys. Lett. A* 165 (1992) 206.
- [87] H. Abreu, H. Hernandez and L. A. Nunez, *Calss. Quantum. Grav.* 24 (2007) 4631.
- [88] S. Chandrasekhar, *Astrophys. J.* 140 (1964) 417.
- [89] H. Bondi, *Proc. R. Soc. Lond. A* 281 (1964) 39.
- [90] R. Chan, L. Herrera, and N. O. Santos, *Mon. Not. R. Astron. Soc.* 265 (1993) 533.
- [91] R. Chan, L. Herrera, and N.O. Santos, *Class. Quantum Grav.* 9 (1992) 133.
- [92] Y. B. Zeldovich, and I. D. Novikov, *Relativistic astrophysics. Vol.1: Stars and relativity*, University of Chicago Press (1971).
- [93] B. K. Harrison, K. S. Thorne, M. Wakano, and J. A. Wheeler, *Gravitation Theory and Gravitational Collapse*, University of Chicago Press (1965).
- [94] B. P. Abbott et al., *Astrophys. J.* 882 (2020) L24.